Acc. Chem. Res. **1999,** *32,* 435−445

Chemistry and Physics in One Dimension: Synthesis and Properties of Nanowires and Nanotubes

JIANGTAO HU, TERI WANG ODOM, AND CHARLES M. LIEBER*

Department of Chemistry and Chemical Biology and Division of Engineering and Applied Sciences, Harvard University, Cambridge, Massachusetts 02138

Received September 24, 1998

I. Introduction

Dimensionality plays a critical role in determining the properties of materials due to, for example, the different ways that electrons interact in three-dimensional, two-dimensional (2D), and one-dimensional (1D) structures.[1−5] The study of dimensionality has a long history in chemistry and physics, although this has been primarily with the prefix "quasi" added to the description of materials; that is, quasi-1D solids, including square-planar platinum chain and metal trichalcogenide compounds,[2,6] and quasi-2D layered solids, such as metal dichalcogenides and copper oxide superconductors.[3−5,7,8] The anisotropy inherent in quasi-1D and -2D systems is central to the unique properties and phases that these materials exhibit, although the small but finite interactions between 1D chains or 2D layers in bulk materials have made it difficult to address the interesting properties expected for the pure low-dimensional systems.

Are pure low-dimensional systems interesting and worth pursuing? We believe that the answer to this question is an unqualified yes from the standpoints of both fundamental science and technology. One needs to look no further than past studies of the 2D electron gas in semiconductor heterostructures, which have produced remarkably rich and often unexpected results,[9,10] and electron tunneling through 0D quantum dots, which have led to the concepts of the artificial atom and the creation of single electron transistors.[11−15] In these cases, low-dimensional systems were realized by creating discrete 2D and 0D nanostructures. 1D nanostructures, such as nanowires and nanotubes, are expected to be at least as interesting and important as 2D and 0D systems.[16,17] 1D systems are the smallest dimension structures that can be used for efficient transport of electrons and optical excitations, and are thus expected to be critical to the function and integration of nanoscale devices. However, little is known about the nature of, for example, localization that could preclude transport through 1D systems. In addition, 1D systems should exhibit density of states singularities, can have energetically discrete molecular-like states extending over large linear distances, and may show more exotic phenomena, such as the spin−charge separation predicted for a Luttinger liquid.[1,2] There are also many applications where 1D nanostructures could be exploited, including nanoelectronics, superstrong and tough composites, functional nanostructured materials, and novel probe microscopy tips.[16−29]

To address these fascinating fundamental scientific issues and potential applications requires answers to two questions at the heart of condensed matter chemistry and physics research: (1) How can atoms or other building blocks be rationally assembled into structures with nanometer-sized diameters but much longer lengths? (2) What are the intrinsic properties of these quantum wires and how do these properties depend, for example, on diameter and structure? Below we describe investigations from our laboratory directed toward these two general questions. The organization of this Account is as follows. In section II, we discuss the development of a general approach to the rational synthesis of crystalline nanowires of arbitrary composition. In section III, we outline key challenges to probing the intrinsic properties of 1D systems and illustrate solutions to these challenges with measurements of the atomic structure and electronic properties of carbon nanotubes. Last, we discuss future directions and challenges in section IV.

II. Synthesis of Nanowires

How can atoms or other building blocks be rationally assembled into structures with nanometer-sized diameters but much longer lengths (1D nanostructures)? There are now well-developed methods for the synthesis of 0D nanoclusters, such as arrested precipitation,[30−32] and for the growth of 2D layers using molecular beam epitaxy.[33] General methods for the growth of 1D nanostructures have not been available, although a number of strategies have been pursued.[16,17] For example, multiwalled carbon nanotubes (MWNTs) have been obtained from hot carbon plasmas.[34,35] The growth mechanism producing MWNTs

Jiangtao Hu was born in Hubei, China. He received his B.S. and M.S. degrees in applied physics from Tsinghua University, and is currently pursuing Ph.D. research with Charles M. Lieber at Harvard University. His research interests center on the growth and properties of new materials.

Teri Wang Odom was born in Novato, CA. She received her B.S. degree in chemistry from Stanford University, and is currently a National Science Foundation Predoctoral Fellow pursuing Ph.D. research with Charles M. Lieber at Harvard University. Her research interests focus on the microscopic properties of low-dimensional materials.

Charles M. Lieber was born in Philadelphia, PA. He received his B.A. and Ph.D. degrees in chemistry from Franklin and Marshall College (1981) and Stanford University (1985), respectively, and was a National Institutes of Health Postdoctoral Fellow at the California Institute of Technology (1985−87). From 1987 until 1991 he was an Assistant Professor and then Associate Professor at Columbia University, and in 1991 moved to Harvard University as a Professor of Chemistry. His research interests center on the chemistry and physics of low-dimensional materials, functional imaging of biological systems, and the development of new techniques to probe inorganic and biological materials on the atomic to nanometer length scales.

10.1021/ar9700365 CCC: $18.00
Published on Web 02/20/1999

under these conditions appears to be specific to the sp^2-bonded carbon and isostructural hexagonal boron nitride,[36,37] although it is possible that other layered materials could form nanotube structures.[38,39] Alternatively, the synthesis of single-walled carbon nanotubes (SWNTs) from carbon plasmas may be favored by adding certain metals.[40−42] These metals appear to function as catalysts, although a sufficiently good understanding of the growth mechanism needed to control the diameter and helicity of SWNTs is not presently available. Templates have also been utilized to direct the growth of 1D nanostructures.[43−47] The nanometer-sized pores in membranes and zeolites have been used to confine the growth of wires,[43,44] and carbon nanotubes have been converted to carbide and nitride nanowires.[45−47] Alternatively, lithography and deposition have been combined to create quantum wires on single-crystal surfaces.[48,49] Template-based techniques are conceptually simple to implement but do have important limitations. For instance, growth in porous membranes typically produces polycrystalline materials with diameters greater than required to observe the effects of quantum confinement. Our goal has been to develop a general and predictive method for preparing compositionally diverse single-crystal materials with nanometer to tens of nanometer diameters in order to understand the intrinsic behavior of 1D structures in a size regime where quantum effects produce new phenomena.

From the outset we believed that a catalytic approach, in which the catalyst is used to direct growth in a highly anisotropic or 1D manner, would enable us to meet this overall goal (Figure 1). Here we envision the catalyst as a cluster that defines the diameter of the structure and localizes the reactant at the end of the growing nanowire much like a catalyst in living polymerization. An important feature of this idea is that it readily provides the intellectual underpinning needed for the prediction of good catalysts and synthesis conditions. First, one uses equilibrium phase diagrams to choose a catalyst that can form a liquid alloy with the nanowire material of interest. The phase diagram is then used to choose a specific composition (catalyst:nanowire material) and synthesis temperature so that there is a coexistence of liquid alloy and solid nanowire material. The liquid catalyst alloy cluster serves as a preferential site for absorption of reactant (i.e., there is a much higher sticking probability on liquid vs solid surfaces) and, when supersaturated, the nucleation site for crystallization. Preferential 1D growth occurs in the presence of reactant as long as the catalyst remains liquid.

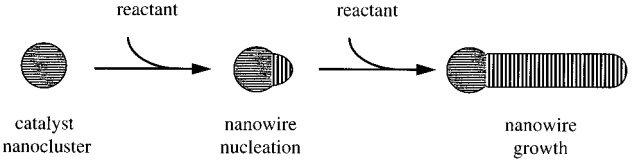

FIGURE 1. Schematic diagram illustrating the catalytic synthesis of nanowires. Reactant material, which is preferentially absorbed on the catalyst cluster, is added to the growing nanowire at the catalyst−nanowire interface.

Within this framework one can readily imagine synthesizing nanowires of many different materials and diameters, if catalyst clusters of nanometer dimensions are available. This raises an important point, because equilibrium thermodynamics can be used to define the minimum radius, r_{min}, of a liquid metal cluster as

$$r_{min} = 2\sigma_{LV}V_L/RT \ln \sigma \quad (1)$$

where σ_{LV} is the liquid−vapor surface free energy, V_L is the molar volume, R and T have the usual meaning, and σ is the vapor phase supersaturation.[50,51] Substituting typical values into eq 1 yields a minimum radius on the order of 0.2 μm, and thus under equilibrium conditions we do not expect to be able to grow nanowires with sufficiently small diameters to exhibit interesting new properties. Indeed, previous studies using a growth process similar to that described above, which is termed vapor−liquid−solid growth in the materials science literature, has only yielded micrometer diameter whiskers.[50,51] The large, ca. micrometer diameter clusters at the ends of these whiskers suggested strongly that the constraint imposed by eq 1 led to the large lower diameter limit in these previous studies. We have overcome this constraint from equilibrium thermodynamics in a general way by employing laser ablation and condensation, which has been studied extensively in the past,[52,53] to generate nanometer diameter clusters. Below we illustrate our general method and its power with examples of the synthesis of elemental and compound nanowire materials.

Consider the synthesis of Si nanowires.[16,17,54,55] The critical catalyst, Si:catalyst composition, and temperature for nanowire growth can be determined by examining the Si-rich region of binary metal−Si phase diagrams. For example, the Fe−Si phase diagram (Figure 2a) tells us that there is a broad area above 1200 °C in the Si-rich region where $FeSi_x$(l) and Si(s) coexist. Within the framework of our approach, Si nanowire synthesis is achieved by laser ablation of a $Si_{0.9}Fe_{0.1}$ target at temperatures ≥1200 °C (Figure 2b,c). Laser ablation of the $Si_{1-x}Fe_x$ target produces a vapor of Si and Fe that rapidly condenses into Si-rich liquid Fe−Si nanoclusters, and when the nanoclusters become supersaturated in Si, the coexisting pure Si phase precipitates and crystallizes as nanowires. Ultimately, the growth terminates when the gas flow carries the nanowires out of the hot zone of the furnace.

Transmission electron microscopy (TEM) studies of the product obtained after laser ablation confirmed these predictions and showed that primarily wire-like structures with remarkably uniform diameters on the order of 10 nm with lengths >1 μm were produced by this approach (Figure 3a). The TEM images recorded on individual nanowires further show that the nanowires consist of very uniform diameter crystalline cores, which are typically 6−20 nm in diameter, surrounded by an amorphous coating (Figure 3b,c). By recording electron diffraction patterns perpendicular to the wire axes and lattice resolved images, it is also possible to determine that the nanowires grow preferentially along the [111] direction at 1200 °C. We elucidated the composition of the core and

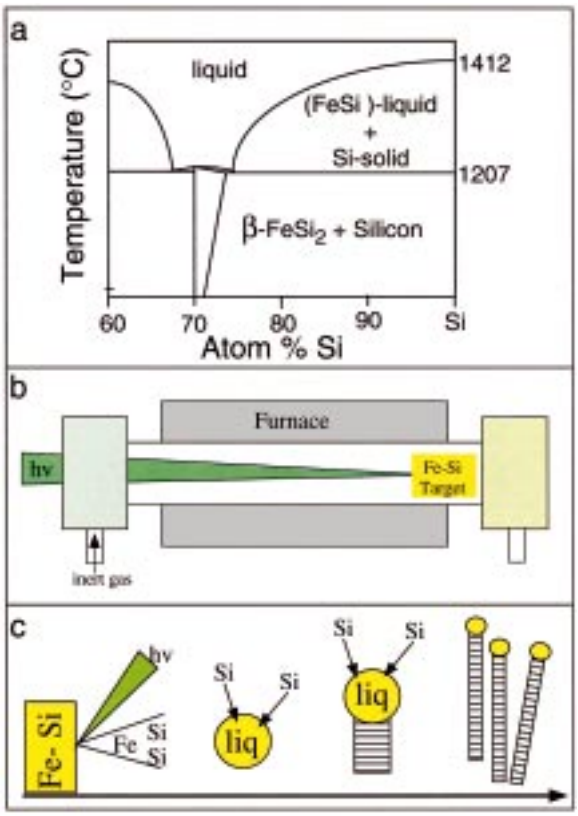

FIGURE 2. (a) Silicon-rich region of the Fe−Si binary phase diagram. (b) Schematic diagram of the nanowire growth apparatus. The output from a pulsed laser is focused onto an Fe−Si target located within a quartz tube; the reaction temperature is controlled by a tube furnace. (c) Nanowire growth process. Laser ablation of the Fe−Si target creates a dense, hot vapor that condenses into nanoclusters as the Fe and Si species cool through collisions with the buffer gas. The furnace temperature is controlled to maintain the Fe−Si nanocluster in a liquid state. Nanowire growth begins after the liquid becomes supersaturated in Si, and continues as long as the Fe−Si nanoclusters remain in a liquid state and Si reactant is available. Growth terminates when the nanowire passes out of the hot zone of the reactor.

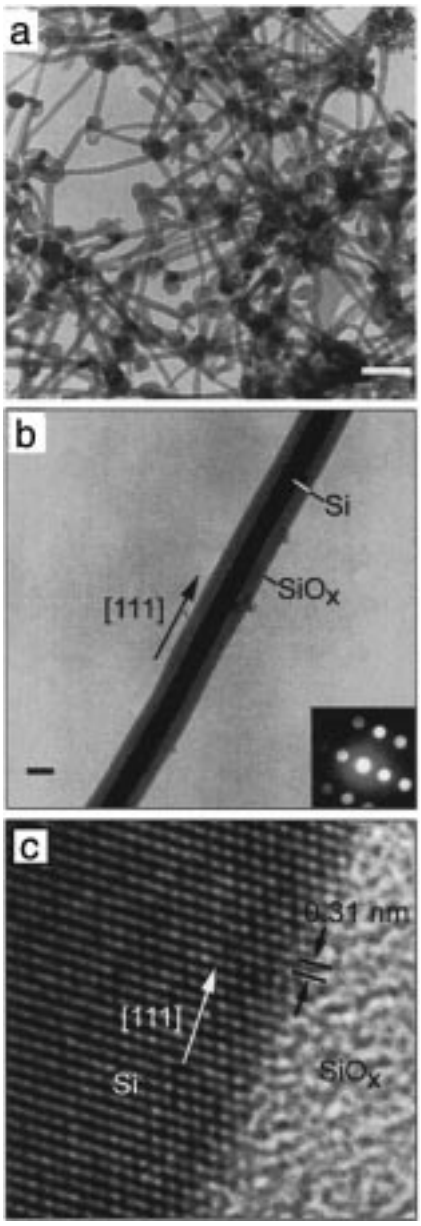

FIGURE 3. (a) TEM image of the nanowires produced following ablation of a $Si_{0.9}Fe_{0.1}$ target. The white scale bar corresponds to 100 nm. (b) Diffraction contrast TEM image of a silicon nanowire Crystalline material (the silicon core) appears darker than amorphous material (SiO_2 sheath) in this imaging mode. The scale bar corresponds to 10 nm. Inset: Electron diffraction recorded along the [211] zone axis. (c) High-resolution TEM image of the crystalline silicon core and amorphous SiO_2 sheath. The (111) planes (spacing 0.31 nm) are oriented perpendicular to the growth direction (white arrow). Reprinted with permission from ref 54. Copyright 1998 American Association for the Advancement of Science.

amorphous sheath using energy-dispersive X-ray (EDX) analysis of individual nanowires before and after etching with HF to remove the amorphous coating. These experiments demonstrate that the crystalline core is pure Si without detectable Fe and that the amorphous coating is SiO_2. Taken together, these data have shown that the nanowires produced using our method consist of single-crystal silicon cores that are surrounded by an amorphous and insulating silicon oxide sheath.[54]

The observation of nanocluster spheres at the ends of the nanowires also provides a strong indication that our overall growth mechanism (Figures 1 and 2c) is correct. One can, of course, provide more detailed support for the mechanism than simply observing clusters at the nanowire ends. Specifically, the Fe−Si phase diagram (Figure 2a) predicts that the terminating solid nanoclusters are $FeSi_2$ and that nanowire growth terminates below ca. 1200 °C. Our quantitative EDX analysis showed that the composition of the clusters at the nanowire ends was $FeSi_2$, and moreover, lattice-resolved TEM images confirmed the crystalline structure of this solid. Last, we found that the growth of the Si nanowires occurred only for temperatures greater than 1150 °C using the Fe catalyst, thus confirming the essential features of our growth model.[54]

The growth of Si nanowires using an Fe catalyst provides a nice illustration of the potential of our approach for the synthesis of crystalline nanowires, but how general is this method? We believe that the synthetic framework outlined above is indeed quite general and can

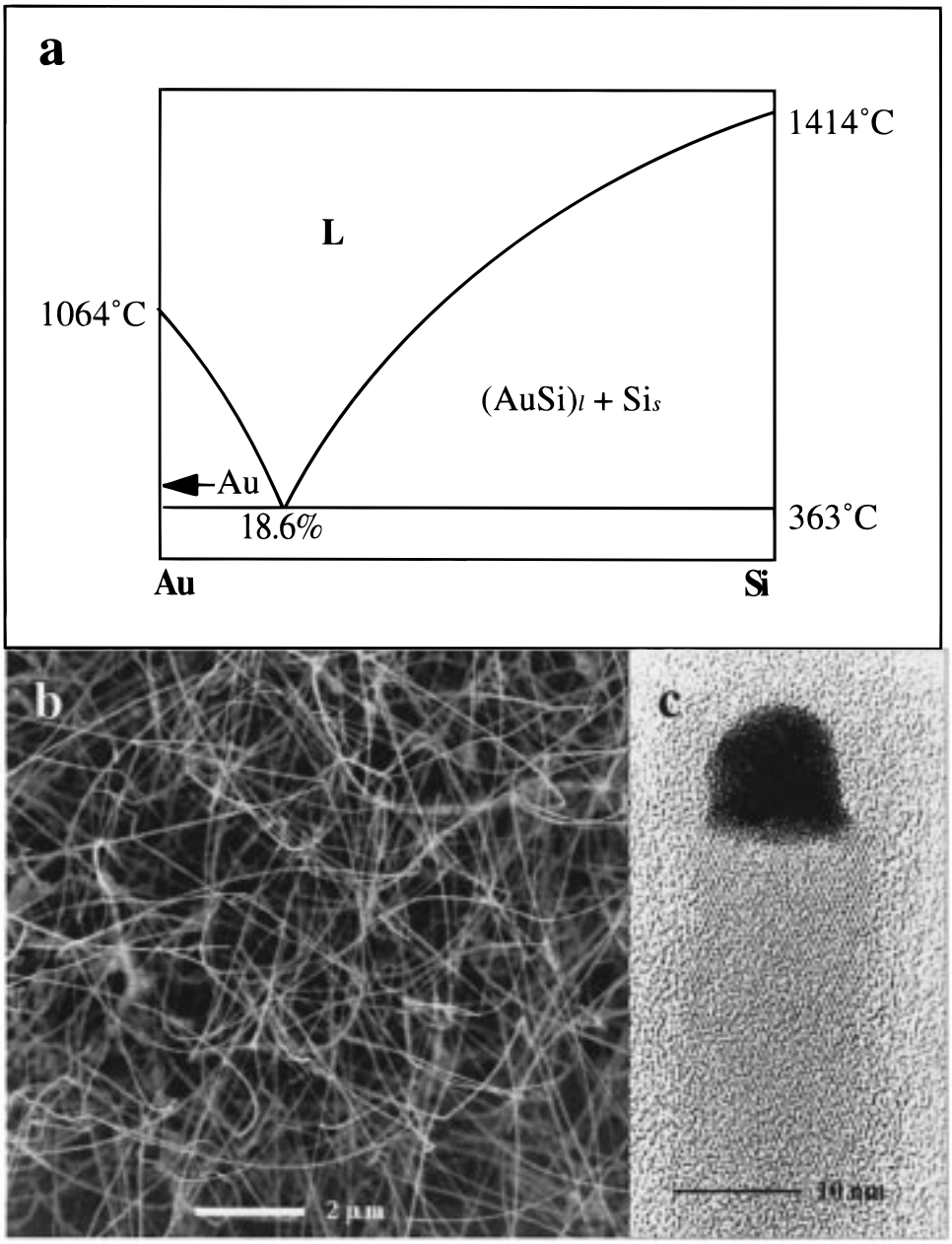

FIGURE 4. (a) Au−Si binary phase diagram. (b) Field-emission scanning electron micrograph of the Si nanowire product produced following ablation of a Au target in the presence of silane at 450 °C. (c) High-resolution TEM image of the end of a 15 nm diameter wire exhibiting Si lattice planes and a gold nanocluster. The Au appears dark in the image.

lead to rapid identification of catalyst materials and growth conditions. We substantiate this claim with several further examples. Maintaining our focus on Si, the predictability afforded by phase diagrams can first be tested by examining different metal catalyst systems. For example, we have studied in some depth the growth of Si nanowires using Au−catalyst nanoclusters, which are produced via ablation of pure gold metal, and the gaseous reactant SiH_4.[55] There are several important results to come from these studies. First, examination of the Au−Si phase diagram (Figure 4a) suggests that nanowire growth via our proposed mechanism should occur at temperatures more than 800 °C lower than in the case of the Fe-based catalyst, and moreover that the solid nanocluster catalyst observed upon termination of growth should be Au metal, not a Au−Si alloy. Our experimental results are in full agreement with these predictions. We have observed facile growth of single-crystal Si nanowires at temperatures between 370 and 500 °C, and found that these wires terminate in Au nanoclusters of similar size (Figure 4b,c). The ability to generate Au nanoclusters independent of Si during ablation and subsequently react these catalyst clusters with the Si reactant (SiH_4) under growth conditions predicted from the Au−Si phase diagram provides unambiguous support for our synthetic model, and has led to the growth of Si nanowires with diameters as small as 3 nm.

The generality of this approach is perhaps best illustrated through the rational synthesis of nanowire materials having different compositions. First, we have

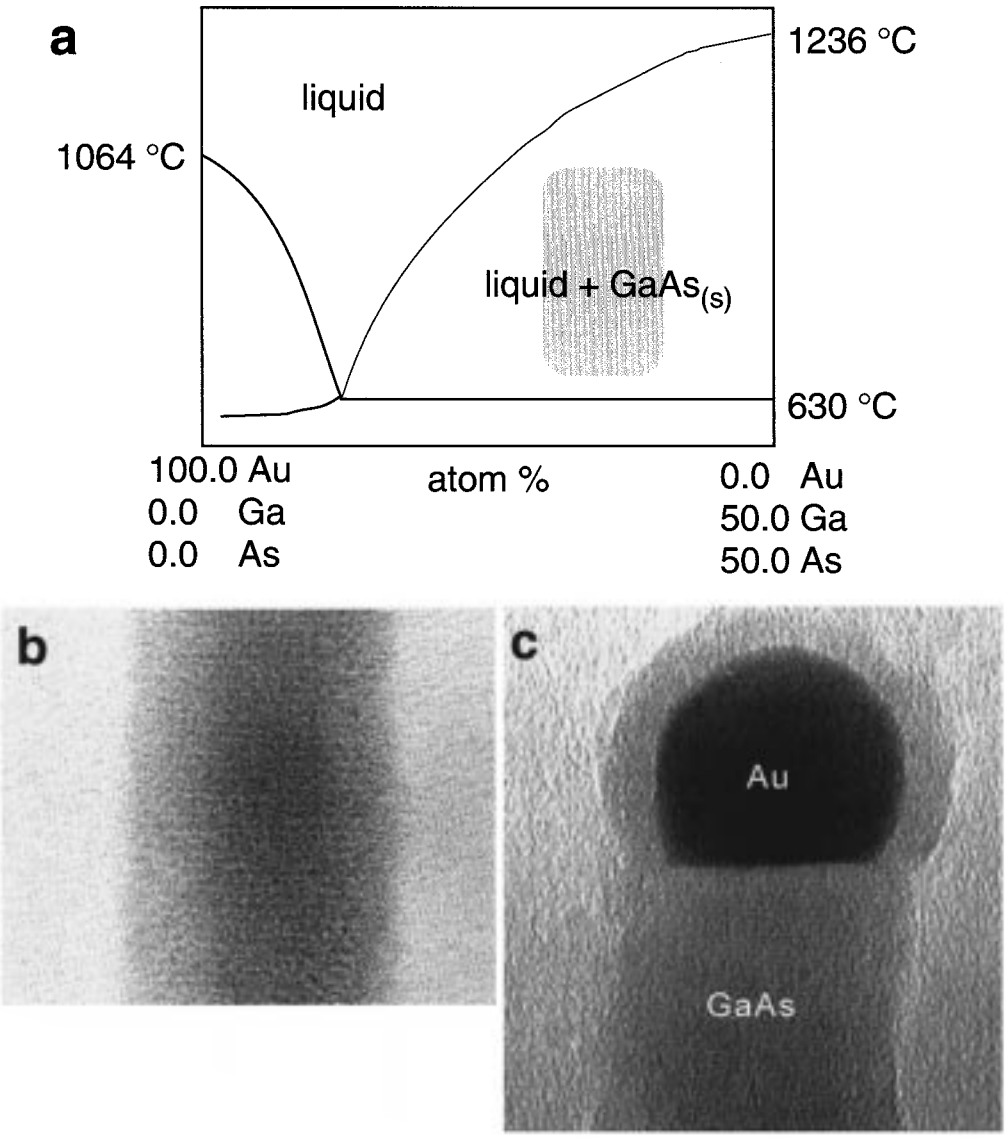

FIGURE 5. (a) Pseudobinary Au−GaAs phase diagram. The shaded area indicates the region of composition and temperature at which the GaAs nanowires were grown. (b) Lattice-resolved TEM image of the body of a 15 nm diameter GaAs nanowire. The (111) lattice planes are perpendicular to the nanowire axis. (c) TEM image showing a Au nanocluster catalyst at the end of the crystalline GaAs nanowire.

prepared single-crystal Ge nanowires with diameters between 3 and 9 nm from Ge−Fe targets in a manner analogous to that for the synthesis of Si nanowires from Si−Fe targets,[54] the major difference in the growth of Ge vs Si nanowires being that the growth temperature is predictably lowered nearly 400 °C (820 vs 1200 °C) on the basis of the eutectic temperature given by the binary Fe−Ge phase diagram.

For a chemist, it is certainly possible to argue that the rational synthesis of Ge nanowires is hardly surprising following our Si nanowire work. However, recent syntheses of a variety of compound semiconductor nanowires are a different story entirely.[56,57] Compound semiconductors, such as GaAs and CdSe, are especially intriguing targets since their direct band gaps afford optical and electrooptical properties that are of considerable importance to basic science and technology. The synthesis of compound semiconductor nanowires using our catalytic approach at first appears a more daunting task when one considers the much greater complexity of ternary versus binary phase diagrams. The analysis of catalyst and growth conditions can be substantially simplified by considering pseudobinary phase diagrams for the metal and compound semiconductor of interest.[56,57] For example, the pseudobinary phase diagrams of GaAs with Cu, Ag, and Au exhibit a large GaAs rich region in which liquid M−GaAs (M = Cu, Ag, Au) coexists with solid GaAs (Figure 5a). Significantly, we have found that single-crystal GaAs nanowires with diameters of a few nanometers and larger can be synthesized in large yield via laser ablation using this information from the phase diagrams to set the catalyst:GaAs composition and growth temperature.[56] Field-emission scanning electron microscopy images show that the GaAs product obtained using a gold catalyst consists almost completely of 1D nanostructures often extending tens of micrometers in length. More detailed

structural analysis has further shown that these nanowires are indeed single crystal in structure and are capped at one end with well-defined Au nanoclusters (Figure 5b,c). The presence of Au nanoclusters at the nanowire ends following the termination of growth is again clear evidence supporting our predictive synthetic model (Figure 1).

We believe it is now possible to exploit this framework for nanowire synthesis to yield a wide range of elemental, binary, and perhaps more complex 1D nanostructures. The crucial points of our approach are that (i) known equilibrium phase diagrams can be used to predict catalyst materials and growth conditions and (ii) laser ablation can be used to generate nanometer-sized diameter clusters of virtually any material, thus enabling rational growth of nanowires of many different materials. We believe that this synthetic approach represents an exciting opportunity for chemists and materials scientists and, moreover, that the properties and applications of these emerging 1D structures will be quite rich.

III. Properties of Quantum Wires

Connecting to the Nanoworld. What are the intrinsic properties of 1D nanostructures, and do they exhibit any novel phenomena? The synthetic studies described above have expanded significantly the availability of 1D nanostructures, and thus offer great opportunity to study how size and dimensionality affect physical properties. Elucidating the intrinsic properties of nanostructures is, however, an experimentally challenging problem in several respects. First, it is necessary to connect from the outside world to the nanometer scale to enable investigations of, for example, electrical conduction and mechanical deformation. Second, nanostructures prepared by either synthesis or fabrication approaches are not identical objects, and typically exhibit dispersions in size and/or structure. Hence, connections to or probes of individual nanostructures offer obvious advantages for elucidating their intrinsic physical properties. This point has been demonstrated clearly in several recent studies, including optical investigations of the luminescence from individual CdSe nanoclusters[59] and scanning tunneling microscopy (STM) studies of the atomic structure and local electronic properties of individual SWNTs.[60−63] In our work, we have exploited scanning probe microscopies, such as STM and atomic force microscopy (AFM), to interrogate the electrical and mechanical properties of individual 1D nanostuctures.[16,17,60,62−66] These techniques provide unique opportunities for defining and uncovering new behavior. Below we focus on relationships of atomic structure and electronic properties of carbon nanotubes probed by STM.

Atomic Structures and Electronic Properties of Carbon Nanotubes. SWNTs represent a unique connection between the molecular and solid state worlds. The structure of SWNTs can be viewed simply as an extension in 1D of different fullerene molecular clusters, and their electronic properties also can be built from relatively simple Hückel-type approaches using only the p(π) atomic orbital on each carbon atom.

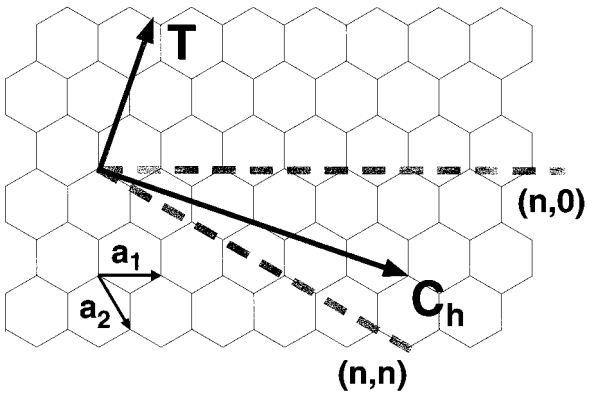

FIGURE 6. Schematic diagram of a 2D graphene sheet illustrating lattice vectors $\mathbf{a}_1$ and $\mathbf{a}_2$, and the roll-up vector $\mathbf{c}_h = n\mathbf{a}_1 + m\mathbf{a}_2$. The limiting cases of (n, 0) zigzag and (n, n) armchair tubes are indicated with dashed lines. The nanotube axis is indicated by the vector **T**.

We can systematically characterize the structures and electronic properties of 1D SWNTs by mentally rolling up a strip cut from an infinite graphene sheet. In particular, the diameter and helicity of a SWNT are uniquely characterized by the vector

$$\mathbf{c}_h = n\mathbf{a}_1 + m\mathbf{a}_2 \equiv (n, m) \qquad (2)$$

that connects crystallographically equivalent sites on this sheet, where $\mathbf{a}_1$ and $\mathbf{a}_2$ are the graphene lattice vectors and n and m are integers (Figure 6). Remarkably, electronic band structure calculations suggested early on that metallic and semiconducting nanotubes should be possible depending only on (n, m);[67−71] that is, subtle variations in structure produce dramatic changes in electronic properties. These calculations suggest that (n, 0) or zigzag SWNTs should exhibit two distinct types of behavior: the tubes will be metals when $n/3$ is an integer, and otherwise semiconductors. As $\mathbf{c}_h$ rotates away from (n, 0), chiral (n, m) SWNTs are possible with electronic properties similar to the zigzag tubes; that is, when $(2n + m)/3$ is an integer, the tubes are metallic, and otherwise semiconducting. Finally, when $\mathbf{c}_h$ rotates 30° relative to (n, 0), n is equal to m and the (n, n) SWNTs are expected to be metallic with band crossings at $\mathbf{k} = \pm 2/3$ of the 1D Brilluoin zone.

Observation of this unique behavior requires that the atomic structure and electronic properties of individual tubes be measured simultaneously, since present methods used to synthesize SWNTs have no control over diameter and helicity (i.e., samples contain tubes with many different (n, m) indices). STM represents an ideal tool for obtaining this critical information. In our initial studies, which were carried out in competition with Cees Dekker's group at Delft (both groups' work published in back to back articles in *Nature*),[60,61] we elucidated the atomic structure of SWNTs supported on Au(111) substrates using a low-temperature, ultrahigh vacuum STM (Figure 7a). Significantly, we showed that high-resolution images of

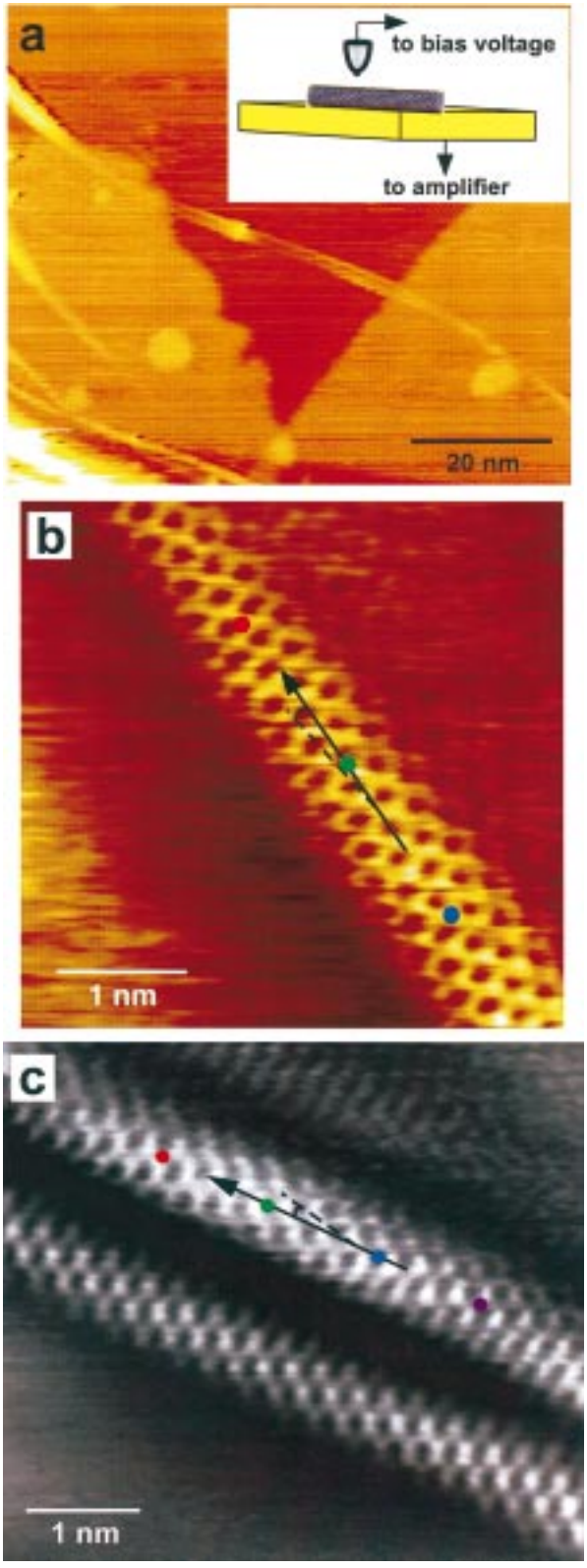

FIGURE 7. (a) Large-area STM image showing several small bundles of SWNTs deposited on a stepped Au(111) surface. The large orange and yellow areas correspond to different height terraces of the Au surface. Inset: Schematic diagram of the STM experiment. (b, c) STM images of SWNTs. The solid, black arrows highlight the tube axes, and the dashed lines indicate the zigzag directions. The images were recorded in the constant-current mode with bias voltages of 50 and 300 mV, respectively, and a tunneling current of 150 pA. The filled, colored circles in (b) and (c) correspond to the locations where $I-V$ data were recorded. Adapted from ref 60.

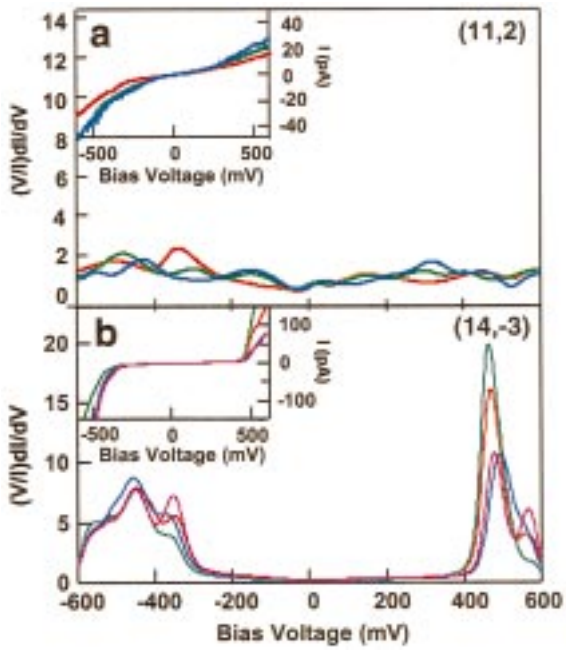

FIGURE 8. (a, b) Calculated normalized conductance, $(V/I)\,dI/dV$, and measured $I-V$ (insets) from the locations indicated in parts b and c, respecively, of Figure 7. The curve colors correspond to the colored circles in parts b and c of Figure 7. Adapted from ref 60.

the nanotubes exhibit a graphite-like honeycomb lattice, thus enabling us to define the (n, m) indices from these images (Figure 7b,c). As an example, the measured chiral angle and diameter of the tube in Figure 7b constrain the (n, m) indices to either (11, 2) or (12, 2). Note that an (11, 2) tube is expected to be metallic, while a (12, 2) tube should be semiconducting. On the other hand, the chiral angle and diameter of the SWNT in Figure 7c constrain the indices to (14, −3) and show that this tube has chirality opposite that of the SWNT in Figure 7b.

The ability to characterize the electronic properties of the atomically resolved tubes by tunneling spectroscopy has enabled us to determine whether the electronic properties depend on structure. Specifically, current (I) vs voltage (V) is measured at specific sites along the SWNTs and differentiated to yield the normalized conductance

$$(V/I)\,dI/dV \equiv \mathrm{LDOS} \qquad (3)$$

which provides a good measure of the local density of electronic states (LDOS). The $I-V$ data that we recorded on the two tubes discussed above exhibit very different characteristics (Figure 8). On the SWNT that we assigned (11, 2) or (12, 2) indices, the current increases with increasing $|V|$, while there is a large voltage region of near zero current for the (14, −3) tube. Similarly, the LDOS determined from these $I-V$ data sets are quite distinct. For the first tube, the LDOS is finite and constant between −600 and +600 mV. This behavior is indicative of a metal. Moreover, the normalized conductance data determined for the (14, −3) tube exhibit an absence of electronic states at low energies but sharp increases in the LDOS at −325 and +425 mV. These sharp increases are characteristic of the conduction and valence band edges of a semiconduc-

tor, and thus confirm our expectation that the (14, −3) indices correspond to a semiconducting SWNT.

The characterization of semiconducting and metallic SWNTs with subtle changes in structure[60,61] confirmed the remarkable electronic behavior of the nanotubes, and represents a significant step forward in understanding these 1D nanostructures. We also believe that this initial work only scratches the surface of a very rich area. The ability to characterize atomic and electronic structures represents a unique opportunity for testing the level of our understanding of the electronic band structure of these 1D materials; for example, can we obtain quantitative agreement between experiment and theory for the 1D singularities in the density of states vs diameter, and interpret the electronic properties of defect and end electronic states, as well as understand the role of symmetry-breaking distortions? Below we look at just one of these issues as an example of the emerging richness of these materials.

The sharp peaks in the DOS that we have determined from our tunneling spectroscopy measurements (e.g., Figure 8b) correspond to van Hove singularities (VHSs) arising from the 1D band structure of the SWNTs.[62,63] These features represent well-defined experimental markers that can, when compared with theory, test and further develop our understanding of the electronic properties of these fascinating materials. For example, chiral SWNTs have unit cells that are typically much larger than the cells of achiral SWNTs of similar diameter, and thus chiral tubes could be expected to exhibit a larger number of VHSs than achiral ones.[72] In contrast, other work has suggested that semiconducting (or metallic) SWNTs of similar diameters will have a similar number of VHSs near the Fermi level, independent of the size of the unit cell.[73] By extending our tunneling spectroscopy measurements to larger energies, we have been able to test these ideas.

In general, $I-V$ data recorded over large voltage ranges on the SWNTs exhibit rich structure.[63] The tunneling current in Figure 9a exhibits relatively sharp, steplike increases at larger $|V|$. At small V, the $I-V$ curves have finite slope, and thus the normalized conductance or LDOS has appreciable nonzero value around $V = 0$ as expected for a metal. This is consistent with the (13, 7) indices determined from the atomic structure of this tube (i.e., $(2n + m)/3$ is an integer). The steplike structure in the $I-V$ curves seen at larger $|V|$, leads to a series of sharp peaks in both dI/dV and the LDOS. These peaks correspond to the VHSs resulting from the extremal points in the 1D energy bands.

We have made a direct comparison of these experimental data to the theoretical electronic band structure calculated within a tight-binding framework (Figure 9b).[63] For example, we calculated the band structure of the (13, 7) SWNT using π and π^* orbitals and zone-folding the 2D graphite band structure into the 1D Brillouin zone specified by the (13, 7) indices. Significantly, our spectroscopy data show good agreement with the calculated DOS for the (13, 7) tube. The agreement between the VHS positions determined from our dI/dV data and calculations is

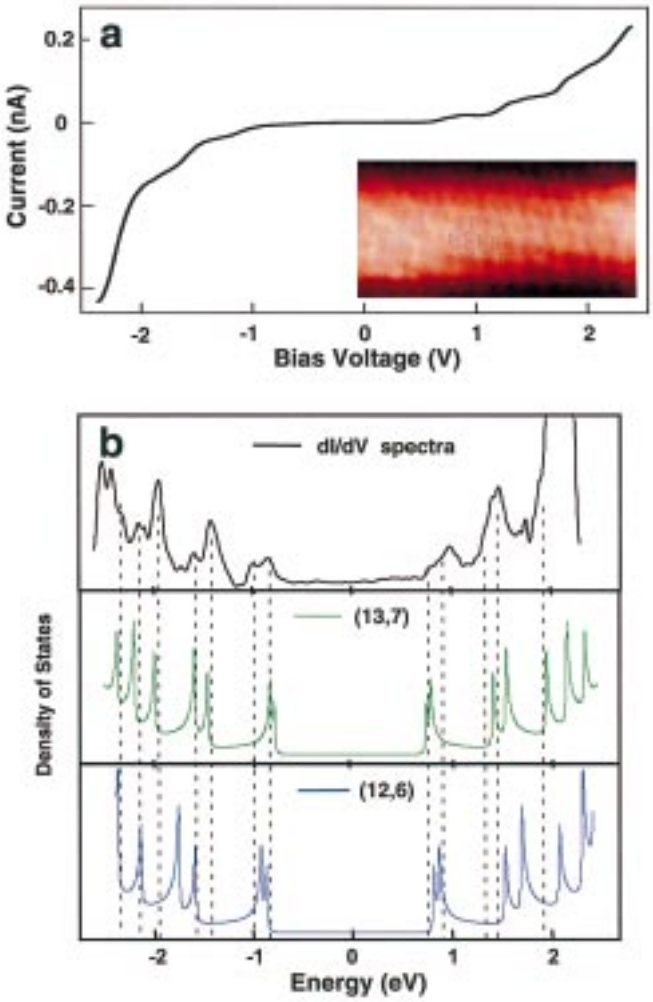

FIGURE 9. (a) $I-V$ data recorded on the (13, 7) SWNT shown in the inset. (b) The top curve shows the conductance calculated from the $I-V$ data in (a). This curve is proportional to the density of states. The middle and bottom plots show the calculated densities of states for (13, 7) and (12, 6) nanotubes, respectively. The densities of states were obtained from a π-only calculation.[63]

especially good below the Fermi energy (E_F) where the first seven peaks correspond well. Above the Fermi energy some deviation between the experimental data and calculations exists. The observed differences may be due to band repulsion, which arises from curvature-induced hybridization. However, a more detailed calculation reported for the (13, 7) tube shows deviations similar to those of our π-only calculation.[74] We have also investigated the sensitivity of the VHSs to variations in the (n, m) indices by calculating the DOS of the next closest metallic SWNT, that is, a (12, 6) tube. It is important to note that the poor agreement in this case demonstrates that subtle variations in diameter and helicity do produce distinguishable changes in the DOS for a given class (metallic or semiconducting) of SWNTs.

These results demonstrate a growing sophistication in our understanding of the electronic structure of these fascinating carbon materials, and we believe that by using STM and other microscopic techniques we have the means to learn much more. For example, it will be

interesting in the future to explore and understand (i) how broken rotational symmetry and mechanical strain affect the low-energy electronic states of SWNTs, (ii) how nanotube−nanotube and nanotube−substrate couplings perturb the electronic properties, (iii) the nature of end states and other finite size effects, and (iv) whether the signatures of a Luttinger liquid can be detected.

IV. Concluding Remarks

In this Account, we have given a brief survey of work, drawn primarily from the authors' laboratory, directed toward understanding the synthesis and properties of 1D nanostructures. Nanowires of a wide range of single-crystal elemental and compound semiconductor materials have now been prepared using a general catalytic synthetic approach. The ability to predict successfully catalyst materials, catalyst:reactant composition, and reaction conditions represents, we believe, a major step forward and makes us confident that nanowire synthesis by design is no longer a dream of the future. STM has also been shown to be a powerful tool for elucidating the structure and electronic properties of 1D nanostructures. By focusing on individual SWNTs within existing heterogeneous samples, we have been able to elucidate their intrinsic properties, thereby demonstrating the remarkable structure−electronic properties of these carbon materials and providing data that have served and are serving to create a much needed dialogue between theory and experiment.

There is, we believe, a very bright future in science and technology for 1D nanostructures. The elemental and compound semiconductor quantum wires emerging from our synthesis represent exciting systems to test fundamental questions about the localization and delocalization of optical excitations in 1D. There remain many fundamental and fascinating issues about the electronic properties of carbon nanotubes and likewise emerging nanowires, such as the coherence of extended states, the role of finite size and symmetry breaking, and new phenomena at low energies, that will require future developments to address. Understanding these points will be critical to many envisioned electronic applications of these 1D materials. We also expect that 1D nanostructures will serve as important building blocks for the assembly of a wide range of functional, nanostructured systems, such as photonic and thermoelectric materials. Ultimately, by cross-cutting ideas and techniques from chemical synthesis, physical chemistry, and physics, we have made and have the opportunity to continue to make quantum jumps forward in our basic understanding of the growth and properties of nanostructures that will define a rich array of technologies in the future.

We thank our co-workers who have made significant contributions to the work described in this Account, including Chin-Li Chueng, Xiangfeng Duan, Jin-Lin Huang, Philip Kim, Alf Morales, and Min Ouyang. C.M.L. also thanks the National Science Foundation, Office of Naval Research, and Air Force Office of Scientific Research for their generous financial support. T.W.O. acknowledges the NSF for a predoctoral fellowship.

References

(1) Voit, J. One-Dimensional Fermi Liquids. *Rep. Prog. Phys.* **1994**, *57*, 977.
(2) See: *Highly Conducting One-Dimensional Solids*; Devreese, J. T., Evrard, R. P., van Doren, V. E., Eds.; Plenum: New York, 1979.
(3) Lieber, C. M.; Wu, X. L. Scanning Tunneling Microscopy Studies of Low-Dimensional Materials: Probing the Effects of Chemical Substitutions at the Atomic Level. *Acc. Chem. Res.* **1991**, *24*, 4, 223.
(4) Dai, H.; Lieber, C. M. Scanning Tunneling Microscopy Studies of Low-Dimensional Materials: Charge Density Wave Pinning and Melting in Two Dimensions. *Annu. Rev. Phys. Chem.* **1993**, *44*, 237.
(5) Lieber, C. M.; Liu, J.; Sheehan, P. E. Understanding and Manipulating Inorganic Materials Using Scanning Probe Microscopes. *Angew. Chem., Int. Ed. Engl.* **1996**, *35*, 686.
(6) See: *Crystal Chemistry and Properties of Materials with Quasi-One-Dimensional Structures*; Rouxel, J., Ed.; Reidel: Boston, 1986.
(7) Wilson, J. A.; DiSalvo, F. J.; Mahajan, S. Charge Density Waves and Superlattices in the Metallic Layered Transition Metal Dichalcogenides. *Adv. Phys.* **1975**, *24*, 117.
(8) Batlogg, B. A. Cuprate Superconductors: Science Beyond High T_c. *Solid State Commun.* **1998**, *107*, 639.
(9) See: *Perspectives in Quantum Hall Effects*; Das-Sarma, S., Pinczuk, A., Eds.; Wiley: New York, 1997.
(10) Stormer, H. L. Fractional Quantum Hall Effect Today. *Solid State Commun.* **1998**, *107*, 617.
(11) See: *Single Charge Tunneling*; Grabert, H., Devoret, M. H., Eds.; Plenum: New York, 1991.
(12) Dvoret, M. H.; Esteve, D.; Urbina, C. Single-Electron Transfer in Metallic Nanostructures. *Nature* **1992**, *360*, 547.
(13) Ashoori, R. C. Electrons in Artificial Atoms. *Nature* **1996**, *379*, 413.
(14) Alivisatos, A. P. Semiconductor Clusters, Nanocrystals, and Quantum Dots. *Science* **1996**, ***271***, 933.
(15) Klein, D. L.; Roth, R.; Lim, A. K. L.; Alivisatos, A. P.; McEuen, P. L. A Single-Electron Transistor Made from a Cadmium Selenide Nanocrystal. *Nature* **1997**, *389*, 699.
(16) Lieber, C. M.; Morales, A. M.; Sheehan, P. E.; Wong, E. W.; Yang, P. One-Dimensional Nanostructures: Rational Synthesis, Novel Properties and Applications. In *Proceedings of the Robert A. Welch Foundation 40th Conference on Chemical Research: Chemistry on the Nanometer Scale*; Welch Foundation: Houston, 1997.
(17) Lieber, C. M. One-Dimensional Nanostructures: Chemistry, Physics & Applications. *Solid State Commun.* **1998**, *107*, 607.
(18) Bockrath, M.; Cobden, D. H.; McEuen, P. L.; Chopra, N. G.; Zettl, A.; Thess, A.; Smalley, R. E. Single-Electron Transport in Ropes of Carbon Nanotubes. *Science* **1997**, *275*, 1922.
(19) Tans, S. J.; Devoret, M. H.; Dai, H.; Thess, A.; Smalley, R. E.; Geerligs, L. J.; Dekker: C. Individual Single-Wall Carbon Nanotubes as Quantum Wires. *Nature* **1997**, *386*, 474.
(20) Tans, S. J.; Verschueren, A. R. M.; Dekker: C. Room-Temperature Transistor Based on a Single Carbon Nanotube. *Nature* **1998**, *393*, 49.
(21) Hu, J.; Ouyang, M.; Yang, P.; Lieber, C. M. Growth and Electrical Properties of Nanotube/Nanowire Heterojunctions. *Nature*, submitted for publication.

(22) Yang, P.; Lieber, C. M. Nanorod-Superconductor Composites: A Pathway to High Critical Current Density Materials. *Science* **1996**, *273*, 1836.
(23) Yang, P.; Lieber, C. M. Columnar Defect Formation in Nanorod/$Tl_2Ba_2Ca_2Cu_3O_z$ Superconducting Composites. *Appl. Phys. Lett.* **1997**, *70*, 3158.
(24) Yang, P.; Lieber, C. M. Nanostructured High-Temperature Superconductors: Creation of Strong-Pinning Columnar Defects in Nanorod/Superconductor Composites. *J. Mater. Res.* **1997**, *12*, 2981.
(25) Dai, H.; Hafner, J. H.; Rinzler, A. G.; Colbert, D. T.; Smalley, R. E. Nanotubes as Nanoprobes in Scanning Probe Microscopy. *Nature* **1996**, *384*, 147.
(26) Wong, S. S.; Harper, J. D.; Lansbury, P. T.; Lieber, C. M. Carbon Nanotube Tips: High-Resolution Probes for Imaging Biological Systems. *J. Am. Chem. Soc.* **1998**, *120*, 603.
(27) Wong, S. S.; Joselevich, E.; Woolley, A. T.; Cheung, C.; Lieber, C. M. Covalently Functionalized Nanotubes as Nanometer Probes for Chemistry and Biology. *Nature* **1998**, *394*, 52.
(28) Wong, S. S.; Woolley, A. T.; Joselevich, E.; Cheung, C.; Lieber, C. M. Covalently-Functionalized Single-Walled Carbon Nanotube Probe Tips for Chemical Force Microscopy. *J. Am. Chem. Soc.* **1998**, *120*, 8557**.**
(29) Wong, S. S.; Woolley, A. T.; Odom, T. W.; Huang, J.-L.; Kim, P.; Vezenov, D. V.; Lieber, C. M. Single-Walled Carbon Nanotube Probes for High-Resolution Nanostructure Imaging. *Appl. Phys. Lett.* **1998**, *73*, 3465.
(30) Murray, C. B.; Norris, D. J.; Bawendi, M. G. Synthesis and Characterization of Nearly Monodisperse CdE (E = S, Se, Te) Semiconductor Nanocrystallites. *J. Am. Chem. Soc.* **1993**, *115*, 8706.
(31) Peng, X.; Schlamp, M. C.; Kadavanich, A. V.; Alivisatos, A. P. Epitaxial Growth of Highly Luminescent CdSe/CdS Core/Shell Nanocrystals with Photostability and Electronic Accessibility. *J. Am. Chem. Soc.* **1997**, *119*, 7019.
(32) Dabbousi, B. O.; Rodriguez-Viejo, J.; Mikulec, F. V.; Heine, J. R.; Mattoussi, H.; Ober, R.; Jensen, K. F.; Bawendi, M. G. (CdSe)ZnS Core−Shell Quantum Dots: Synthesis and Characterization of a Size Series of Highly Luminescent Nanocrystallites. *J. Phys. Chem. B* **1997**, *101*, 9463.
(33) See: Herman, M. A.; Sitter, H. *Molecular Beam Epitaxy*; Springer: New York, 1989.
(34) Colbert, D. T.; Zhang, J.; McClure, S. M.; Nikolaev, P.; Chen, Z.; Hafner, J. H.; Owens, D. W.; Kotula, P. G.; Carter, C. B.; Weaver, J. H.; Rinzler, A. G.; Smalley, R. E. Growth and Sintering of Fullerene Nanotubes. *Science* **1994**, *266*, 1218.
(35) Ebbesen, T. W.; Ajayan, P. M. Large-Scale Synthesis of Carbon Nanotubes. *Nature* **1992**, *358*, 220.
(36) Chopra, N. G.; Luyken, R. J.; Cherrey, K.; Crespi, V. H.; Cohen, M. L.; Louie, S. G.; Zettl, A. Boron Nitride Nanotubes. *Science* **1995**, *269*, 966.
(37) Terrones, M.; Hsu, W. K.; Terrones, H.; Zhang, J. P.; Ramos, S.; Hare, J. P.; Castillo, R.; Prassides, K.; Cheetham, A. K.; Kroto, H. W.; Walton, D. R. M. Metal Particle Catalysed Production of Nanoscale BN Structures. *Chem. Phys. Lett.* **1996**, *259*, 568.
(38) Tenne, R.; Margulis, L.; Genut, M.; Hodes, G. Polyhedral and Cylindrical Structures of Tungsten Disulfide. *Nature* **1992**, *360*, 444.
(39) Feldman, Y.; Wasserman, E.; Srolovitz, D. J.; Tenne, R. High-Rate, Gas-Phase Growth of MoS_2 Nested Inorganic Fullerenes and Nanotubes. *Science* **1995**, *267*, 222.
(40) Iijima, S.; Ichihashi, T. Single-Shell Carbon Nanotubes of 1 nm Diameter. *Nature* **1993**, *363*, 603.
(41) Bethune, D. S.; Kiang, C. H.; de Vries, M. S.; Gorman, G.; Savoy, R.; Vazquez, J.; Beyers, R. Cobalt-Catalyzed Growth of Carbon Nanotubes with Single Atomic Layer Walls. *Nature* **1993**, *363*, 605.
(42) Thess, A.; Lee, R.; Nikolaev, P.; Dai, H.; Petit, P.; Robert, J.; Xu, C.; Lee, Y. H.; Kim, S. G.; Rinzler, A. G.; Colbert, D. T.; Scuseria, G. E.; Tomanek, D.; Fischer, J. E.; Smalley, R. E. Crystalline Ropes of Metallic Carbon Nanotubes. *Science* **1996**, *273*, 483.
(43) Martin, C. R. Nanomaterials: A Membrane-Based Synthetic Approach. *Science* **1994**, *266*, 1961.
(44) Wu, C.-G.; Bein, T. Conducting Carbon Wires in Ordered, Nanometer-Sized Channels. *Science* **1994**, *266*, 1013.
(45) Dai, H.; Wong, E. W.; Lu, Y. Z.; Fan, S.; Lieber, C. M. Synthesis and Characterization of Carbide Nanorods. *Nature* **1995**, *375*, 769.
(46) Wong, E. W.; Maynor, B. W.; Burns, L. D.; Lieber, C. M. Growth of Metal Carbide Nanotubes and Nanorods. *Chem. Mater.* **1996**, *8*, 2041.
(47) Han, W. Q.; Fan, S. S.; Li, Q. Q.; Hu, Y. D. Synthesis of Gallium Nitride Nanorods Through a Carbon Nanotube-Confined Reaction. *Science* **1997**, *277*, 1287.
(48) Namatsu, H.; Kurihara, K.; Nagase, M.; Makino, T. Fabrication of 2 nm Wide Silicon Quantum Wires Through a Combination of a Partially-Shifted Resist Pattern and Orientation-Dependent Etching. *Appl. Phys. Lett.* **1997**, *70*, 619.
(49) Wang, J.; Thompson, D. A.; Robinson, B. J.; Simmons, J. G. Molecular Beam Epitaxial Growth of InGaAs/InGaAsP Quantum Wires on V-grooved InP Substrates with (111) Sidewalls. *J. Cryst. Growth* **1997**, *175*, 793.
(50) Wagner, R. S.; Ellis, W. C. Vapor-Solid-Growth Mechanism of Single Crystal Growth. *Appl. Phys. Lett.* **1964**, *4*, 89.
(51) Wagner, R. S. VLS Mechanism of Crystal Growth. In *Whisker Technology*; Levitt, A. P., Ed.; Wiley: New York, 1970.
(52) Dietz, T. G.; Duncan, M. A.; Powers, D. E.; Smalley, R. E. Laser Production of Supersonic Metal Cluster Beams. *J. Chem. Phys.* **1981**, *74*, 6511.
(53) See: El-Shall, M. S.; Edelstein, A. S. Formation of Clusters and Nanoparticles from a Supersaturated Vapor and Selected Properties. In *Nanomaterials: Synthesis, Properties and Applications*; Edelstein, A. S., Cammarata, R. C., Eds.; Institute of Physics: Philadelphia, 1996.
(54) Morales, A. M.; Lieber, C. M. A Laser Ablation Method for the Synthesis of Crystalline Semiconductor Nanowires. *Science* **1998**, *279*, 208.
(55) Hu, J.; Duan, X.; Lieber, C. M. Unpublished results.
(56) Duan, X.; Hu, J.; Lieber, C. M. Unpublished results.
(57) Duan, X.; Lieber, C. M. Unpublished results.
(58) Panish, M. B. Ternary Condensed Phase Systems of Gallium and Arsenic with Group IB Elements. *J. Electrochem. Soc.* **1967**, *114*, 516.
(59) Empedocles, S. A.; Norris, D. J.; Bawendi, M. G. Photoluminescence Spectroscopy of Single CdSe Nanocrystallite Quantum Dots. *Phys. Rev. Lett.* **1996**, *77*, 3873.
(60) Odom, T. W.; Huang, J.-L.; Kim, P.; Lieber, C. M. Atomic Structure and Electronic Properties of Single-Walled Carbon Nanotubes. *Nature* **1998**, *391*, 62.
(61) Wildoer, J. W. G.; Venema, L. C.; Rinzler, A. G.; Smalley, R. E.; Dekker, C. Electronic Structure of Atomically Resolved Carbon Nanotubes. *Nature* **1998**, *391*, 59.

(62) Odom, T. W.; Huang, J.-L.; Kim, P.; Ouyang, M.; Lieber, C. M. Scanning Tunneling Microscopy and Spectroscopy Studies of Single Wall Carbon Nanotubes. *J. Mater. Res.* **1998**, *13*, 2380.
(63) Kim, P.; Odom, T. W.; Huang, J.-L.; Lieber, C. M. Electronic Density of States of Atomically-Resolved Single-Walled Carbon Nanotubes: Van Hove Singularities and End States. *Phys. Rev. Lett.* **1999**, *82*, 1225.
(64) Zhang, J.; Liu, J.; Huang, J.-L.; Lieber, C. M. Creation of Nanocrystals via a STM Tip-Induced Solid−Solid-Phase Transition. *Science* **1996**, *274*, 757.
(65) Dai, H.; Wong, E. W.; Lieber, C. M. Probing Electrical Transport in Nanomaterials: Conductivity of Individual Carbon Nanotubes. *Science* **1996**, *272*, 523.
(66) Wong, E. W.; Sheehan, P. E.; Lieber, C. M. Nanobeam Mechanics: Elasticity, Strength and Toughness of Nanorods and Nanotubes. *Science* **1997**, *277*, 1971.
(67) Mintmire, J. W.; Dunlap, B. I.; White, C. T. Are Fullerene Tubules Metallic? *Phys. Rev. Lett.* **1992**, *68*, 631.
(68) Hamada, N.; Sawada, S.; Oshiyama, A. New One-Dimensional Conductors: Graphitic Microtubules. *Phys. Rev. Lett.* **1992**, *68*, 1579.
(69) Saito, R.; Fujita, M.; Dresselhaus, G.; Dresselhaus, M. S. Electronic Structure of Chiral Graphene Tubules. *Appl. Phys. Lett.* **1992**, *60*, 2204.
(70) Saito, R.; Fujita, M.; Dresselhaus, G.; Dresselhaus, M. S. Electronic Structure of Graphene Tubules Based on C_{60}. *Phys. Rev. B* **1992**, *46*, 1804.
(71) White, C. T.; Robertson, D. H.; Mintmire, J. W. Helical and Rotational Symmetries of Nanoscale Graphitic Tubules. *Phys. Rev. B* **1993**, *47*, 5485.
(72) Dresselhaus, M. S. New Tricks with Nanotubes. *Nature* **1998**, *391*, 19.
(73) White, C. T.; Mintmire, J. W. Density of States Reflects Diameter in Nanotubes. *Nature* **1998**, *394*, 29.
(74) Charlier, J.-C.; Lambin, Ph. Electronic Structure of Carbon Nanotubes with Chiral Symmetry. *Phys. Rev. B* **1998**, *57*, R15037.

AR9700365